A "MORPHOLOGICAL APPROACH" FOR MODELLING THE ELASTIC AND VISCOELASTIC PROPERTIES OF STRAND-BASED WOOD COMPOSITES: COMPARISON WITH OTHER RECENT ANALYTICAL AND NUMERICAL MODELS

Malekmohammadi[a], B. Tressou[b], C. Nadot-Martin[b*], R. Vaziri[a]

[a] *Composites Group, Departments of Civil Engineering and Materials Engineering, The University of British Columbia, Vancouver, BC, V6T 1Z4, Canada*
[b] *Département Physique et Mécanique des Matériaux, Institut Pprime (UPR 3346 CNRS – ENSMA – Université de Poitiers), Poitiers, France*
[*]*carole.nadot@ensma.fr*

Keywords: parallel strand lumber, scale transition, analytical models, full-field finite element simulations, orthotropic properties.

Abstract

Strand-based wood composites, such as parallel strand lumber (PSL), are increasingly being used in construction of mid-rise buildings. These composites consist of orthotropic wood strands covered with small amount of resin. In order to estimate the effective properties of these materials, a specific scale transition approach, called "Morphological approach" (MA), is employed. The latter has been shown to be particularly effective for highly-filled composites in previous studies devoted to another class of materials. In this paper, the accuracy of the MA in estimating the effective properties of a unit cell of a PSL beam is investigated by comparison with reference solutions obtained by full-field Finite Element (FE) simulations. The MA is also compared to another recent analytical scale transition approach used for strand-based wood composites. First, this is done considering both constituents (strands and resin) linear elastic and then considering the viscoelasticity of the resin. In both cases, MA results are shown to be closer to the numerical reference solutions than other analytical estimates.

1. Introduction

The motivation for this work comes from structural wood composite industry. Strand-based wood composites are a new category of building materials that are widely being used in the construction industry, especially in North America. This type of material which belongs to a class of wood-based composites made of wood strands is becoming popular in other parts of the world due to its reasonable cost compared to conventional construction materials, environmental friendliness and tailorable properties.

Strand-based wood composites (e.g. Parallel Strand Lumber or PSL) consist of high volume fractions of fully orthotropic fibres (wood strands) bonded together with a thermoset resin (e.g. Phenol Formaldehyde). Resin content is usually less than 5% by weight and strands are close to being rectangular in shape, due to the cutting method widely used in the wood composite industry.

In this paper a specific scale transition approach, devoted to highly filled particulate composites, and called “Morphological Approach” (MA) is applied to estimate elastic and viscoelastic properties of a PSL unit cell. In a general manner, the MA is based on an explicit representation of the material morphology in which each particle (here strand) and each resin inter-granular region is labelled and characterized with morphological parameters. This allows taking into account salient features such as spatial arrangement and morphology of constituents in addition to volume fractions. Thanks to a specific kinematical description, the MA faces the crucial challenge of accounting for strong and complex interactions between opposite particles when the matrix volume fraction is low. Strong subsequent effects on the global non-linear behavior of a composite may thus be correctly described for a low computational effort, *e.g.* see [1], [2], [3].

The objective is to evaluate the relevance of the MA as applied to PSL materials. To this aim, the MA estimates are compared to full-field finite element reference solutions and to recent analytical estimates proposed by [4]. This is done for a wide range of resin content, as used in wood composite industry.

2. Real mesostructure and idealization

A typical sample of PSL, which is used as beams and columns in wood frame buildings, is shown in Figure 1. As in in the recent work by Malekmohammadi et al. [4], the strand-based composite structure is here idealized as a regular assembly of rectangular strands with the same size and covered by a thin layer of resin with constant thickness. With such representation, we may define a unit cell of the material as shown in Figure 1. The strand thickness, width and length are chosen to be 5mm, 13mm and 600mm, respectively. These values are taken from the experimental study conducted by [5]. As in the work by Gereke et al. [6], it is moreover assumed that PSL is free of voids and that there is perfect bonding between strands and resin. Analytical estimates resulting from MA and [4], as well as FE reference solutions, will be based on this idealization of the real mesostructure.

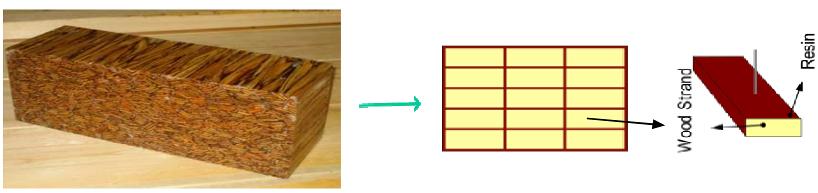

Figure 1. Sample of a PSL, idealized mesotructure and unit cell definition, [4]

3. Principle of the “Morphological approach”

3.1 Generalities for any highly-filled particulate composite, [1]

The initial microstructure of a highly-filled composite is represented by an aggregate of polyhedral grains interconnected by thin matrix layers with constant thicknesses. This schematization is illustrated in Figure 2. In the case of a particulate composite, a numerical polyhedrization process is applied to this aim. For each layer α, four morphological parameters are then identified (Figure 2c):

- h^{α}, the constant thickness of layer α
- A^{α}, the projected area of layer α; the associated volume is then $A^{\alpha} h^{\alpha}$
- $\boldsymbol{d}^{\alpha}$, the vector linking the centroids of the polyhedra separated by layer α
- $\boldsymbol{n}^{\alpha}$, the unit vector normal to the plane interface grain/layer α.

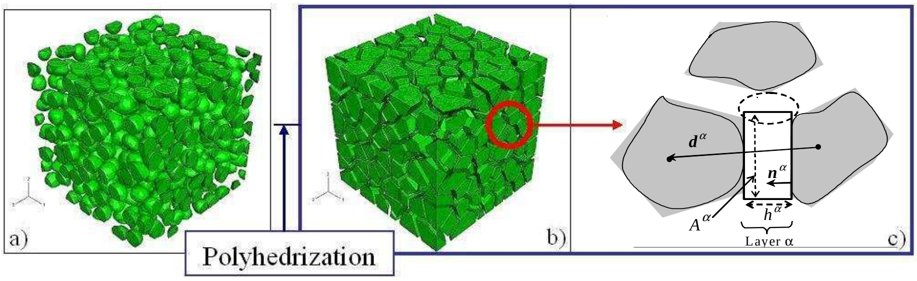

Figure 2. Illustration of the geometrical schematization, [1]: a) real particulate composite microstructure, b) schematized microstructure, c) morphological parameters for a layer α (2D representation)

Once the grains are replaced by polyhedra (satisfying the condition of parallelism between the interfaces of opposite grains), the parameters $\boldsymbol{d}^{\alpha}$, $\boldsymbol{n}^{\alpha}$, h^{α} and A^{a} are readily determined thanks to simple geometrical measurements.

The local problem approach is based on simplifying assumptions regarding the local displacement in the schematized volume. The grain centroids are displaced so as to conform to a global, homogeneous displacement gradient $\boldsymbol{F}$ (characterizing the imposed loading). The grains are supposed homogeneously deformed and the corresponding displacement gradient $\boldsymbol{f}^{0}$ assumed to be identical for all grains. Each interconnecting layer is subjected to a homogeneous displacement gradient, proper to the layer α considered and noted $\boldsymbol{f}^{\alpha}$. Local disturbances at grain edges and corners (circled zone, Figure 2c) are neglected on the basis of thinness of the layers.

With these assumptions, the continuity of displacements on the grain/layer interfaces leads to the expression of the displacement gradient $\boldsymbol{f}^{\alpha}$ of any layer α as a function of the macroscopic gradient $\boldsymbol{F}$, of $\boldsymbol{f}^{0}$ and of the morphological parameters proper to the layer, (see [1], [2] for more details):

$$f_{ij}^{\alpha} = f_{ij}^{0} + \left(F - f^{0} \right)_{ik} \frac{d_k^{\alpha} n_j^{\alpha}}{h^{\alpha}} \tag{1}$$

The compatibility between local motion defined above and the global motion characterized by the given displacement gradient $\boldsymbol{F}$, (*i.e.* $\boldsymbol{F} = \langle \boldsymbol{f} \rangle_{|V|}$) is ensured through the following condition to be satisfied by the morphological parameters of the schematized material:

$$\frac{1}{|V|} \sum_{\alpha} d_i^{\alpha} n_j^{\alpha} A^{\alpha} = \delta_{ij} \tag{2}$$

where $|V|$ is the volume of the assembly of grains and layers and δ_{ij} is the Kronecker symbol. Then, the Hill-Mandel principle of macro-homogeneity applied in the context considered (*i.e.* by using (1) and (2)), gives rise to the following equation:

$$(1-c)\sigma_{ij}^{0}+\frac{1}{|V|}\sum_{\alpha}\sigma_{ij}^{\alpha}A^{\alpha}h^{\alpha}-\frac{1}{|V|}\sum_{\alpha}\sigma_{ki}^{\alpha}n_{k}^{\alpha}A^{\alpha}d_{j}^{\alpha}=0 \qquad (3)$$

$\boldsymbol{\sigma}^{0}$ and $\boldsymbol{\sigma}^{\alpha}$ denote the average Cauchy stress tensors over the grains and layer α, respectively. $c=\frac{1}{|V_0|}\sum_{\alpha}A^{\alpha}h^{\alpha}$ is the layers' concentration with respect to volume $|V|$.

3.2 Solving procedure

Consider a schematized volume satisfying the compatibility requirement (2) and a loading path characterized by the macroscopic displacement gradient $\boldsymbol{F}$. The input data for the local problem are thus $\boldsymbol{F}$, morphological parameters $\left\{\boldsymbol{d}^{\alpha},\boldsymbol{n}^{\alpha},h^{\alpha},A^{\alpha}\ \ \forall\alpha\right\}$ and constituents' mechanical properties. The local constitutive laws for the grain and matrix are introduced in (3) as well as (1) to explicit $\boldsymbol{f}^{\alpha}$. Then, Equation (3) is solved to give $\boldsymbol{f}^{0}$ as a function of input data. The knowledge of $\boldsymbol{f}^{0}$ allows the backwards calculation of the composite response at both scales: $\boldsymbol{f}^{\alpha}$ for any layer α by using (1), local stresses by the local laws and finally the homogenized Cauchy stress tensor $\boldsymbol{\Sigma}$ by volume averaging. This solving strategy is valid whatever the constituents' laws.

3.3 Case of linear elasticity

In the elastic case and whatever the constituents' material symmetries, the solving procedure is analytical and leads to the following expression of the homogenized stiffness tensor, *[2]*:

$$\boldsymbol{L}^{Hom}=\left\langle \boldsymbol{L}^{(e)}\right\rangle_{|V|}-\boldsymbol{A}:\boldsymbol{B}^{-1}:\boldsymbol{A} \qquad (4)$$

where:

$$\boldsymbol{A}=\left\langle \boldsymbol{L}^{(e)}\right\rangle_{|V|}-\boldsymbol{L}^{(e)Matrix} \qquad (5)$$

$$B_{ijkl}=A_{ijkl}-L_{ijkl}^{(e)Matrix}+L_{mjnl}^{(e)Matrix}\overline{T}_{imkn} \qquad (6)$$

$$\overline{T}_{ijkl}=\frac{1}{|V|}\sum_{\alpha}d_{i}^{\alpha}\,n_{j}^{\alpha}\,d_{k}^{\alpha}\,n_{l}^{\alpha}\,A^{\alpha}/h^{\alpha} \qquad (7)$$

$\left\langle \boldsymbol{L}^{(e)}\right\rangle_{|V|}$ designates the volume average of the local stiffness tensor and $\boldsymbol{L}^{(e)Matrix}$ the matrix stiffness tensor. It is stressed that the MA accounts for initial morphology and internal organization of constituents through the presence of the fourth-order structural tensor $\overline{\boldsymbol{T}}$ given by (7) in the expression of the homogenized stiffness tensor (via $\boldsymbol{B}$). The reader may refer to the work by [7] where it is shown that $\overline{\boldsymbol{T}}$ reflects possible material texture and irregularities in grain shape and in layer thickness.

3.4 Case of linear viscoelasticity

When the matrix is linear viscoelastic defined by Prony series expansions, Equation (3) is numerically solved using a Newton-Raphson algorithm. It is to be noted that the solving is direct, namely it is performed in the real time domain without using Laplace transforms. This is a crucial difference with Eshelby-based homogenization methods. Previous works [1] have shown the ability of MA to deal with complex spatio-temporal local interactions between constituents and subsequent macroscopic effect called "Long memory effect".

Relaxation loading paths for each of the six classical elementary loadings are imposed to the schematized volume in order to compute the effective stiffness tensor at each time step and finally deduce the time evolution of engineering constants.

4. MA application to a PSL and results

4.1 Morphological parameters identification

The idealized mesostructure presented in Figure 1 respects by nature the requirements of the geometrical schematization recalled in Section 3.1. Moreover, considering the periodicity it is sufficient to consider as domain V for which Equation (3) is solved, only one rectangular grain (strand) and three layers: "layer i" for i = 1,2,3, with respective normal unit vector $\boldsymbol{n}^i = \boldsymbol{i}$ as illustrated in Figure 3. The intergranular distance being the same in the three directions, the layers have identical thickness (h). The norms d^i of vectors $\boldsymbol{d}^i = d^i\,\boldsymbol{i}$ are deduced from the knowledge of h and dimensions of the strand. The projected areas A^i are calculated so that the condition (2) is exactly satisfied. The values of (h, d^i and A^i for i = 1,2,3) are different for each resin volume fraction that will be considered in the following section.

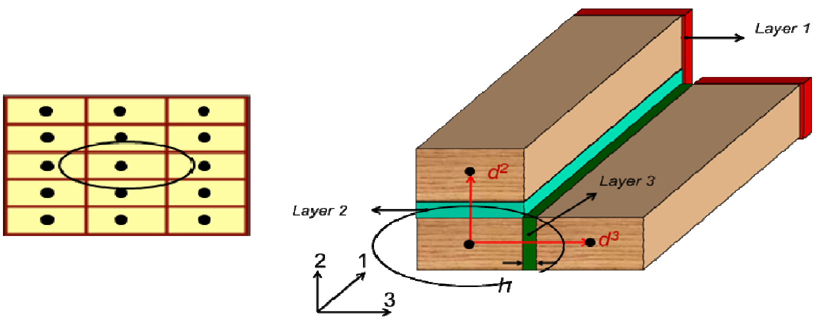

Figure 3. Idealized PSL mesotructure and elementary "pattern" for MA with morphological characteristics parameters

4.2 Results in elasticity

The elastic properties of resin and wood strand used in both numerical and analytical approaches are listed in Table 1. Resin is assumed to be isotropic and elastic in this section. The elastic properties of Phenol Formaldehyde (PF) resin are taken from the literature [8].

The orthotropic elastic properties of strands are those of Pine wood taken from wood handbook [9].

Material	Young's Modulus (GPa)			Shear Modulus (GPa)			Poisson's ratio		
	E_1	E_2	E_3	G_{12}	G_{13}	G_{23}	ν_{12}	ν_{13}	ν_{23}
Wood	13	1.393	0.856	0.991	0.909	0.162	0.467	0.456	0.488
Resin		7.6			2.92			0.3	

Table 1. Constituents' elastic properties

Figure 4 shows the comparison between the analytical and numerical results for different resin volume fractions. MA estimates are in better agreement with FE reference solutions than estimates due to [4], noted (Ana) in Figure 4. The relative error between MA estimates and reference solutions remains below 0.8% while it is 5% for the estimates due to [4].

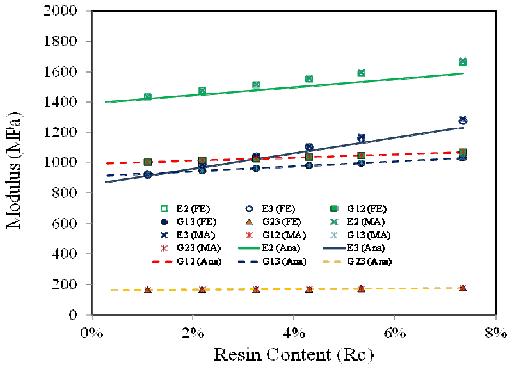

Figure 4. Comparison of homogenized moduli obtained by the MA and the previous approach due to Malekmohammadi et al. [4] to FE reference solutions, for different resin volume fractions

4.3 Results in viscoelasticity

The geometrical and mechanical characteristics of the strand are the same as for elastic analysis. The resin content is 7.3% by volume corresponding to resin thickness h of 0.28 mm. The resin phase shear and bulk moduli (G and K, respectively) are defined by Prony series expansions following the classical formulation available in Abaqus®. The series for the shear and bulk moduli are distributed over five relaxation times ranging over four decades. Shear weight factors g_k and associated relaxation times τ_k are taken from the literature [10]. Elastic properties given in Table 1 are used for the instantaneous, unrelaxed, shear and bulk modulus values. Since the bulk modulus of the resin is difficult to measure during relaxation, identical distributions are prescribed (g_k = k_k). The resulting parameters defining the Prony series are given in Table 2. It should be noted that the viscoelastic behaviour of the PF resin used in wood composite industry may be different from the data given in Table 2. However, using the same Prony series for both numerical and analytical approaches is sufficient to evaluate analytical estimates by comparison with numerical reference data.

No.	g_k	k_k	τ_k (sec)
1	0.171479	0.171479	1.01E-02
2	0.0833645	0.0833645	1.01E-01
3	0.0348822	0.0348822	1.01E+00
4	0.0120372	0.0120372	1.01E+01
5	0.698237	0.698237	1.01E+02

Table 2. Resin viscoelastic properties (Prony series parameters for the shear and bulk moduli)

As an illustration of the results, Figure 5 shows the comparison between the analytical and numerical results for transverse Young's moduli. Once again MA estimates are better than estimates obtained by previous work due to [4].

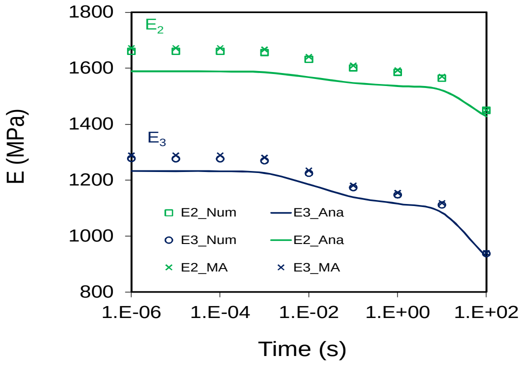

Figure 5. Comparison of transverse relaxation moduli obtained by the MA and the work due to Malekmohammadi et al. [4] to FE reference solutions, for resin volume fraction equal to 7.3%

References

[1] C. Nadot-Martin, M. Touboul, A. Dragon and A. Fanget. Direct scale transition approach for highly-filled viscohyperelastic particulate composites: computational study. [In] Multiscale Modeling of Heterogeneous Materials: From Microstructure to Macro-scale Properties, O. Cazacu ed., ISTE/Wiley, 218-237, 2008.

[2] C. Nadot, A. Dragon, H. Trumel and A. Fanget. Damage modelling framework for viscoelastic particulate composites via a scale transition approach. *Journal of Theoretical and Applied Mechanics*, 44(3), 553-583, 2006.

[3] S. Dartois, C. Nadot-Martin, D. Halm, A. Dragon, A. Fanget and G. Contesse. Micromechanical modelling of damage evolution in highly-filled particulate composites - Induced effects at different scales. *International Journal of Damage Mechanics*, 22(7), 927-966, 2013.

[4] S. Malekmohammadi, B. Tressou, C. Nadot-Martin, F. Ellyin, R. Vaziri. Analytical micromechanics equations for elastic and viscoelastic properties of strand-based composites. *Journal of Composite Materials*, DOI: 10.1177/0021998313490977, 2013.

[5] S.R. Arwade, P.L. Clouston, R. Winans. Measurement and Stochastic Computational Modeling of the Elastic Properties of Parallel Strand Lumber. *Journal of Engineering Mechanics-ASCE*, 135(9), 897-905, 2009.

[6] T. Gereke, S. Malekmohammadi, C. Nadot-Martin, C. Dai, F. Ellyin, R. Vaziri. Multi-Scale Stochastic Modeling of the Elastic Properties of Strand-Based Wood Composites. *Journal of Engineering Mechanics*, 138(7), 791-799, 2012.

[7] J. Christoffersen. Bonded granulates. *Journal of Mechanics and Physics Solids*, 31, 55-83, 1983.

[8] S.M. Shaler, P.R. Blankenhorn. Composite Model Prediction of Elastic-Moduli for Flakeboard. *Wood and Fiber Science*, 22(3), 246-261, 1990.

[9] T. Nishimura, J. Amin, M. Ansell. Image analysis and bending properties of model OSB panels as a function of strand distribution, shape and size. *Wood Science and Technology*, 38(4), 297-309, 2004.

[10] A. Naik, N. Abolfathi, G. Karami, G. Ziejewski. Micromechanical Viscoelastic Characterization of Fibrous Composites. *Journal of Composite Materials*, 42(12), 1179-1204, 2008.